J. Fluid Mech. (1993), vol. 247, pp. 503–525

Effects of Görtler vortices, wall cooling and gas dissociation on the Rayleigh instability in a hypersonic boundary layer

By YIBIN FU AND PHILIP HALL
Department of Mathematics, University of Manchester, Manchester M13 9PL, UK

(Received 24 January 1992 and in revised form 10 August 1992)

In a hypersonic boundary layer over a wall of variable curvature, the region most susceptible to Görtler vortices is the temperature adjustment layer sitting at the edge of the boundary layer. This temperature adjustment layer is also the most dangerous site for Rayleigh instability. In this paper, we investigate how the existence of large-amplitude Görtler vortices affects the growth rate of Rayleigh instability. The effects of wall cooling and gas dissociation on this instability are also studied. We find that all these mechanisms increase the growth rate of Rayleigh instability and are therefore destabilizing.

1. Introduction

Curved surfaces are unavoidable in many engineering designs. The engine inlets and the control surfaces of hypersonic vehicles are examples. Peculiar to curved surfaces is the Görtler instability mechanism which can be induced by wall curvature. In this paper, we continue our systematic studies on the Görtler instability mechanism in the hypersonic context. The starting point of our present study is the nonlinear theory presented in our previous paper (Fu & Hall 1992). In that paper we have shown that when Görtler vortices evolve downstream of the neutral position, a large-amplitude vortex structure can be established under the combined action of nonlinearity and viscosity. This structure consists of a region of vortex activity bounded by two viscous transition layers over which the vortices are reduced to zero exponentially. Above the upper transition layer and below the lower transition layer there is only the mean flow. The determination of the locations of the two transition layers gives rise to a free boundary problem which we have solved for different curvature distributions. After such a large-amplitude Görtler vortex structure has been established, various travelling waves may be triggered in the form of secondary instabilities. Experimental results given by Swearingen & Blackwelder (1987) suggest that at least two forms of secondary instabilities may exist. The first instability is located at the two transition layers, $\frac{1}{2}\pi$ out of phase in the spanwise direction with the existing Görtler vortices and thus leads to wavy vortex boundaries. The other possible instability is in phase with the existing Görtler vortices and has an inviscid nature. Thus it is a Rayleigh instability. In our previous paper (Fu & Hall 1992), the wavy type of instability has been fully studied and we have shown that a family of neutral travelling wave modes may exist. In the present paper, we shall investigate the Rayleigh secondary instability which the large Görtler vortex structure may suffer.

The present secondary instability problem can also be interpreted in the following way. It has been shown in Hall & Fu (1989) and Fu, Hall & Blackaby (1992) that in a hypersonic boundary layer over a wall of variable curvature, the region most susceptible to Görtler vortices is the temperature adjustment layer sitting at the edge of the boundary layer. This temperature adjustment layer is also the most dangerous site for Rayleigh instability, as has been shown by Cowley & Hall (1990), Smith & Brown (1990), and Blackaby, Cowley & Hall (1993). It is therefore of interest to investigate how Görtler vortices interact with Rayleigh travelling waves in the temperature adjustment layer. Of greater importance is the question of whether the existence of Görtler vortices in the boundary layer makes the layer more susceptible to a Rayleigh instability. It has been established in Fu & Hall (1992) that as Görtler vortices develop downstream of the neutrally stable location, nonlinear effects produce a mean flow correction as large as the original basic state. Thus at locations $O(1)$ downstream of the neutral position, the original basic state is completely altered by Görtler vortices. Our main concern in this paper is to understand how such alterations of the basic state by Görtler vortices affect the growth rate of Rayleigh instability.

The other problems which we consider here are the influences of gas dissociation and wall cooling on Rayleigh instability in the temperature adjustment layer. The influence of gas dissociation does not seem to have been studied before in the large Mach number limit, whilst the influence of wall cooling has previously been examined by Blackaby *et al.* (1993), but their analysis is for unit Prandtl number. Here we shall re-examine this problem for Prandtl number equal to 0.72 which is more relevant to air.

This paper is organized as follows. In the next section, we state our problem and give asymptotic solutions for the basic state, whilst in §3 we describe the large-amplitude Görtler vortex structure and the resulting mean flow. The numerical solution of the latter is then discussed in §4, in preparation for the solution of Rayleigh equation. In §5, we first formulate the Rayleigh instability problem and then study the influence of wall cooling and gas dissociation on the Rayleigh modes in the absence of Görtler vortices. Finally we investigate the influence of Görtler vortices on Rayleigh modes. We discuss our numerical results and then draw some conclusions.

2. The original basic state

Consider a hypersonic boundary layer over a rigid wall of variable curvature $(1/A)\,\kappa(x^*/L)$, where L is a typical streamwise lengthscale and A is a lengthscale characterizing the radius of curvature of the wall. We choose a curvilinear coordinate system (x^*, y^*, z^*) with x^* measuring distance along the wall, y^* perpendicular to the wall and z^* in the spanwise direction. The corresponding velocity components are denoted by (u^*, v^*, w^*) and density, temperature and viscosity by ρ^*, T^* and μ^* respectively. The free-stream values of these quantities will be signified by a subscript ∞. The Reynolds number R, the curvature parameter Δ and the Görtler number G are defined by

$$R = u^*_\infty L\rho^*_\infty/\mu^*_\infty, \quad \Delta = L/A, \quad G = 2R^{\frac{1}{2}}\Delta. \tag{2.1}$$

We assume that the Reynolds number is large, while Δ is taken to be small. In the context of incompressible flows, the characteristic values of G for instability are $O(1)$; whilst in hypersonic flows G is $O(M^2)$ when Chapman's viscosity law is used (see Hall & Fu 1989), and is $O(M^{\frac{3}{2}})$ when Sutherland's viscosity law is used (see Fu *et al.* 1992).

In the following analysis, coordinates (x^*, y^*, z^*) are scaled on $(L, R^{-\frac{1}{2}}L, R^{-\frac{1}{2}}L)$, the velocity (u^*, v^*, w^*) is scaled on $(u^*_\infty, R^{-\frac{1}{2}}u^*_\infty, R^{-\frac{1}{2}}u^*_\infty)$ and other quantities such as ρ^*, T^*, and μ^* are scaled on their free-stream values with the only exception that the pressure p^* is scaled on $\rho^*_\infty u^{*2}_\infty$ and the bulk viscosity is scaled on μ^*_∞. (Such a scaling is only appropriate to the Görtler problem and in the Rayleigh problem to be discussed in §5 a different scaling will be used.) All dimensionless quantities will be denoted by the same letters without a superscript *. Then the Navier–Stokes and energy equations and the equation of state are, to leading order, given by

$$\frac{\partial \rho}{\partial t}+\frac{\partial}{\partial x_\beta}(\rho v_\beta) = 0, \tag{2.2}$$

$$\rho\frac{\mathrm{D}u}{\mathrm{D}t} = -\frac{\partial p}{\partial x}+\frac{\partial}{\partial y}\left(\mu\frac{\partial u}{\partial y}\right)+\frac{\partial}{\partial z}\left(\mu\frac{\partial u}{\partial z}\right), \tag{2.3}$$

$$\rho\frac{\mathrm{D}v}{\mathrm{D}t}+\tfrac{1}{2}G\kappa u^2 = -R\frac{\partial p}{\partial y}+\frac{\partial}{\partial y}\left\{(\lambda-\tfrac{2}{3}\mu)\frac{\partial v_\beta}{\partial x_\beta}\right\}+\frac{\partial}{\partial x_\beta}\left(\mu\frac{\partial v_\beta}{\partial y}\right)+\frac{\partial}{\partial y}\left(\mu\frac{\partial v}{\partial y}\right)+\frac{\partial}{\partial z}\left(\mu\frac{\partial v}{\partial z}\right), \tag{2.4}$$

$$\rho\frac{\mathrm{D}w}{\mathrm{D}t} = -R\frac{\partial p}{\partial z}+\frac{\partial}{\partial z}\left\{(\lambda-\tfrac{2}{3}\mu)\frac{\partial v_\beta}{\partial x_\beta}\right\}+\frac{\partial}{\partial x_\beta}\left(\mu\frac{\partial v_\beta}{\partial z}\right)+\frac{\partial}{\partial y}\left(\mu\frac{\partial w}{\partial y}\right)+\frac{\partial}{\partial z}\left(\mu\frac{\partial w}{\partial z}\right), \tag{2.5}$$

$$\rho c_p\frac{\mathrm{D}T}{\mathrm{D}t} = \mu(\gamma-1)M^2\left[\left(\frac{\partial u}{\partial y}\right)^2+\left(\frac{\partial u}{\partial z}\right)^2\right]+(\gamma-1)M^2\left[1-\rho\left(\frac{\partial h}{\partial p}\right)_T\right]\frac{\mathrm{D}p}{\mathrm{D}t}$$
$$+\frac{1}{\sigma}\frac{\partial}{\partial y}\left(k\frac{\partial T}{\partial y}\right)+\frac{1}{\sigma}\frac{\partial}{\partial z}\left(k\frac{\partial T}{\partial z}\right), \tag{2.6}$$

$$\gamma M^2 p = (1+\alpha)\rho T. \tag{2.7}$$

Here terms of relative order $R^{-\frac{1}{2}}$ have been neglected and we have used a mixed notation in which (v_1, v_2, v_3) is identified with (u, v, w) and (x_1, x_2, x_3) with (x, y, z). Repeated suffices β signify summation from 1 to 3. The functions λ, k, c_p and h denote in turn the bulk viscosity, the coefficient of heat conduction, the specific heat at constant pressure and the enthalpy per unit mass. The constants γ, M and σ are in turn the ratio of specific heats, the Mach number and the Prandtl number defined by

$$\gamma = \frac{c_{p_\infty}}{c_{v_\infty}}, \quad M^2 = \frac{u^{*2}_\infty}{\gamma\Re T^*_\infty} = \frac{u^{*2}_\infty}{a^2_\infty}, \quad \sigma = \frac{\mu_\infty c_{p_\infty}}{k^*_\infty},$$

where $\Re$ is the gas constant and $a_\infty = (\gamma\Re T^*_\infty)^{\frac{1}{2}}$ is the sound speed in the free stream. Finally, the function α in the equation of state (2.7) denotes the percentage by mass of the mixture which has been dissociated. (We assume that the gas in an ideal diatomic gas, say A_2. After dissociation has taken place, each A_2 molecule dissociates into two A atoms and the gas becomes a gas mixture of A_2 and A.) In (2.3)–(2.6), the operator $\mathrm{D}/\mathrm{D}t$ is the material derivative and it has the usual expression appropriate to a rectangular coordinate system. If gas dissociation is neglected, the above governing equations can be simplified by putting $\alpha = 0$, $c_p = 1$ and $(\partial h/\partial p)_T = 0$.

The basic state is given by

$$(u, v, w) = (\bar{u}(x,y), \bar{v}(x,y), 0), \quad T = \bar{T}(x,y), \quad \rho = \bar{\rho}(x,y), \quad \mu = \bar{\mu}(x,y). \tag{2.8}$$

By substituting (2.8) into the governing equations (2.2)–(2.7) it is straightforward to obtain the reduced equations satisfied by the basic state. The reader is referred to the book by Stewartson (1964) for a detailed discussion of these equations. If we define the Howarth–Dorodnitsyn variable $\bar{y}$ and a similarity variable η by

$$\bar{y} = \int_0^y \bar{\rho}\,\mathrm{d}y \quad \text{and} \quad \eta = \frac{\bar{y}}{(2x)^{\frac{1}{2}}}, \tag{2.9}$$

then the continuity equation is satisfied if $\bar{u}$ and $\bar{v}$ are written as

$$\bar{u} = f'(\eta), \quad \bar{v} = \frac{1}{(2x)^{\frac{1}{2}}}\left[-\frac{1}{\bar{\rho}}f(\eta) + f'(\eta)\int_0^\eta \frac{1}{\bar{\rho}}\,\mathrm{d}\eta\right]. \tag{2.10}$$

Here the functions $f(\eta)$ and $\bar{T}(\eta)$ must satisfy

$$ff'' + (\bar{\rho}\bar{\mu}f'')' = 0, \tag{2.11}$$

$$(1/\sigma)(\bar{\rho}\bar{k}\bar{T}')' + \bar{c}_p f\bar{T}' + \mu(\gamma-1)M^2\bar{\rho}(f'')^2 = 0, \tag{2.12}$$

if the x-momentum and energy equations are to be satisfied. These equations must then be solved such that f, f' vanish at the wall, $f', \bar{T} = 1$ at infinity and either $\bar{T}' = 0$ or $\bar{T}$ specified at the wall. The y-momentum equation gives

$$\partial\bar{p}/\partial y = 0$$

to leading order so that $\bar{p} = \bar{p}(x)$. In the following analysis, we assume that there is no pressure gradient along the streamwise direction and therefore we can take $\bar{p}$ = constant. Equation (2.7) then gives

$$[1 + \alpha(\bar{T})]\bar{\rho}\bar{T} = 1. \tag{2.13}$$

In the Görtler problem, the pressure perturbation is $O(1/R)$ relative to the unperturbed pressure and therefore the above relation for the basic state can be extended to

$$[1 + \alpha(T)]\rho T = 1, \tag{2.14}$$

which is valid for the total flow (as long as M^2/R is small).

We now give a summary of the asymptotic solutions of the basic state equations (2.11) and (2.12) for an *ideal dissociating gas*. A detailed derivation of these results can be found in Fu *et al.* (1992). The corresponding results for an ideal *undissociated* gas can be obtained by putting $\alpha = 0$ in the following equations.

An ideal dissociating gas is a diatomic gas which satisfies the following dissociation law:

$$\frac{\alpha^2}{1-\alpha^2} = \frac{p_\mathrm{d}}{p}\frac{T}{T_\mathrm{d}}\mathrm{e}^{-T_\mathrm{d}/T} \tag{2.15}$$

(see Lighthill 1957, p. 6 or Becker 1968, p. 36). Here p_d and T_d are respectively the *characteristic pressure* and *temperature* for dissociation. On rewriting this relation in terms of non-dimensional variables and using the fact that $\bar{p}$ is a constant, we have

$$\frac{\alpha^2}{1-\alpha^2} = \frac{\rho_\mathrm{d}}{\rho_\infty}\bar{T}\mathrm{e}^{-T_\mathrm{d}/T_\infty\bar{T}}, \tag{2.16}$$

where $\rho_d = p_d/(\Re T_d)$ is the *characteristic density* for dissociation. For the purpose of asymptotic analysis, it is convenient to define two new constants a and b by

$$a = \frac{\rho_d}{\rho_\infty} M^2, \quad b = \frac{T_d}{T_\infty M^2}. \tag{2.17}$$

Then (2.16) becomes

$$\frac{\alpha^2}{1-\alpha^2} = \frac{a\bar{T}}{M^2} e^{-bM^2/\bar{T}}, \tag{2.18}$$

which displays the physical fact that dissociation will take place in the hottest region where $\bar{T} = O(M^2)$.

We assume that after dissociation each component of the gas mixture has its viscosity given by Sutherland's law. We further assume that the viscosity of the gas mixture is described by Wilke's law and the coefficient of heat conduction given by Wassiljewa's formula. It can be shown that in the large Mach number limit, the boundary layer splits into two sublayers: a wall layer and a temperature adjustment layer. In the wall layer, $\eta \sim M^{-\frac{1}{2}}$, $\bar{T} \sim M^2$, $f \sim M^{-\frac{1}{2}}$, so it is appropriate to define $O(1)$ variables Y, $\tilde{T}$ and $F(Y)$ by

$$Y = M^{\frac{1}{2}}\eta, \quad \tilde{T} = M^{-2}\bar{T}, \quad F(Y) = M^{\frac{1}{2}}f. \tag{2.19}$$

Then (2.11) and (2.12) give

$$(1+m)\left(\frac{h_1(\alpha)}{1+\alpha}\frac{F''}{\tilde{T}^{\frac{1}{2}}}\right)' + FF'' = 0, \tag{2.20}$$

$$\frac{1+m}{\sigma}\left(\frac{h_2(\alpha)}{1+\alpha}\frac{\tilde{T}'}{\tilde{T}^{\frac{1}{2}}}\right)' + \bar{c}_p F\tilde{T}' + (\gamma-1)(1+m)\frac{h_1(\alpha)}{1+\alpha}\frac{(F'')^2}{\tilde{T}^{\frac{1}{2}}} = 0, \tag{2.21}$$

where

$$h_1 \stackrel{\text{def.}}{=} \frac{\tilde{A}_3(1-\alpha)}{2\alpha+\tilde{A}_3(1-\alpha)} + \frac{\tilde{A}_2\tilde{A}_3\,\alpha}{\tilde{A}_3\,\alpha+\tilde{A}_2(1-\alpha)}, \tag{2.22}$$

$$h_2 \stackrel{\text{def.}}{=} \frac{\tilde{A}_3(1-\alpha)}{2\alpha+\tilde{A}_3(1-\alpha)} + \frac{(10\tilde{A}_2\tilde{A}_3/7)\,\alpha}{\tilde{A}_3\,\alpha+\tilde{A}_2(1-\alpha)}, \tag{2.23}$$

$$\bar{c}_p = 1 + \frac{1}{4}\alpha + \frac{1}{8}\left(1+\frac{b}{\tilde{T}}\right)^2 \alpha(1-\alpha^2). \tag{2.24}$$

Here $\tilde{A}_2, \tilde{A}_3$ are constants which appear in Wilke's law and m is the constant appearing in Sutherland viscosity law for the undissociated gas. On rewriting (2.18) in terms of $\tilde{T}$, we have

$$\frac{\alpha^2}{1-\alpha^2} = a\tilde{T}\, e^{-b/\tilde{T}}. \tag{2.25}$$

Equations (2.20)–(2.25) are to be solved numerically subject to the conditions

$$\left.\begin{array}{l} F(0) = F'(0) = 0, \quad \tilde{T}(\infty) = 0, \quad F'(\infty) = 1, \\ \tilde{T}'(0) = 0 \text{ if the wall is thermally insulated,} \\ \tilde{T}(0) = n\tilde{T}_w \text{ if the wall is under cooling,} \end{array}\right\} \tag{2.26}$$

where $\tilde{T}_w$ is the wall temperature scaled on $M^2 T_\infty$ when the wall is thermally insulated and n is the wall cooling coefficient.

As $Y \to \infty$, $\tilde{T} \to 0$ and α decays to zero exponentially. From (2.22)–(2.24) we have $h_1 \to 1$, $h_2 \to 1$ and $\bar{c}_p \to 1$. Thus as the edge of the boundary layer is approached, the effects of gas dissociation become negligible and (2.20) and (2.21) can then be approximated by

$$(1+m)(F''/\tilde{T}^{\frac{1}{2}})'+FF''=0, \tag{2.27}$$

$$\frac{1+m}{\sigma}\left(\frac{\tilde{T}'}{\tilde{T}^{\frac{1}{2}}}\right)'+F\tilde{T}'+(\gamma-1)(1+m)\frac{(F'')^2}{\tilde{T}^{\frac{1}{2}}}=0, \tag{2.28}$$

which have asymptotic solutions

$$F=Y-\beta+\frac{D}{(Y-\beta)^{3/\sigma}}+\dots,\quad \tilde{T}=\left[\frac{3(1+m)}{\sigma}\right]^2\frac{1}{(Y-\beta)^4}+\dots, \tag{2.29}$$

where both D and β are constants. In the temperature adjustment layer $\eta=O(1)$, there is no dissociation and in order to match with (2.29), the solutions for f and $\bar{T}$ must expand as

$$f=\eta-\frac{\beta}{M^{\frac{1}{2}}}+\frac{\hat{f}(\eta)}{M_1}+\dots, \tag{2.30}$$

$$\bar{T}=\hat{T}(\eta)+\dots. \tag{2.31}$$

Here M_1 is defined by $\qquad M_1=M^{\frac{3}{2\sigma}+\frac{1}{2}}.$

On substituting (2.30) and (2.31) into (2.11) and (2.12), we obtain to leading order

$$(1+m)\left(\frac{\hat{T}^{\frac{1}{2}}}{\hat{T}+m}\hat{f}''\right)'+\eta\hat{f}''=0, \tag{2.32}$$

$$\frac{(1+m)}{\sigma}\left(\frac{\hat{T}^{\frac{1}{2}}}{\hat{T}+m}\hat{T}'\right)'+\eta\hat{T}'=0. \tag{2.33}$$

These two equations are to be solved numerically subject to the matching conditions

$$\text{as } \eta\to 0,\quad \hat{f}(\eta)\sim\frac{D}{\eta^{3/\sigma}},\quad \hat{T}\sim\frac{9(1+m)^2}{\sigma^2}\frac{1}{\eta^4}+\dots, \tag{2.34}$$

and at infinity $\qquad \hat{f}'(\infty)=0,\quad \hat{T}(\infty)=1. \qquad (2.35)$

It can be shown from (2.32) and (2.33) that

$$\hat{f}''(\eta)=\frac{D}{(1+m)^{1+1/\sigma}}\left(\frac{\sigma}{12}\right)^{1/\sigma}\left(\frac{3}{\sigma}+1\right)\left(\frac{\hat{T}+m}{\hat{T}^{\frac{1}{2}}}\right)^{1-1/\sigma}(-\hat{T}')^{1/\sigma}, \tag{2.36}$$

so that after (2.33) has been solved numerically, the function $\hat{f}''(\eta)$ can be computed easily from this equation. Also, we note that whilst the solution of (2.33) is independent of the wall-layer solutions and thus of the conditions at the wall, the function $\hat{f}$ is dependent on the wall-layer solutions through the matching constant D. As will be shown later, D is an important constant and it is through this constant that the influence of wall cooling and gas dissociation affect the growth rate of Rayleigh instability in the temperature adjustment layer. In table 1, we show the dependence

	$n = 0.2$	$n = 0.4$	$n = 0.6$	$n = 0.8$	$n = 1$
Ideal gas	395	313	257	216	186
Real gas	405	326	271	232	206

TABLE 1. Dependence of D on gas dissociation and wall cooling

of D on wall cooling and gas dissociation. In our numerical integration of the boundary layer equations (2.20) and (2.21), we have taken $\sigma = 0.72$, $m = 0.508$, $\gamma = 1.4$, $\tilde{A}_2 = \tilde{A}_3 = 1$, $a = 1.21 \times 10^9$, $b = 3.30$. As a check, we have also used our program to obtain the value of D when $\sigma = 1$, the wall insulated and gas dissociation neglected, for which the exact solution for D is possible and is given by

$$D = \frac{3(1+m)^2}{\gamma - 1}. \tag{2.37}$$

Our numerical solution yields $D = 17.02$, whilst (2.37) gives $D = 17.08$.

3. The large Görtler vortex structure

Because of the curvature of the wall, the hypersonic boundary layer described in the previous section may lose stability to Görtler vortices. In the linear Görtler instability analysis, we are concerned with the determination of the conditions under which Görtler vortices grow in the streamwise direction. To this end, we superimpose on the basic state (2.8) a steady periodic stationary vortex structure with wavenumber a in the spanwise direction and the perturbation equations are found by linearizing the governing equations about the basic state. These linear equations have been fully discussed in our previous paper Fu *et al.* (1992). It was shown there that for the wall-layer mode which has wavelength comparable with the boundary-layer thickness, the neutral Görtler number is a decreasing function of the local wavenumber. As the latter increases, the centre of vortex activity moves towards the temperature adjustment layer and the Görtler number tends to a constant which is the leading-order term in the Görtler number expansion for the mode trapped in the temperature adjustment layer. It is this mode that is most susceptible to Görtler vortices since it has a smaller Görtler number than any other mode.

As is typical of Görtler vortices in growing boundary layers, the evolution of Görtler vortices in the temperature adjustment layer is dominated by non-parallel effects. It was shown in Fu *et al.* (1992) that in the hypersonic limit such non-parallel effects operate mainly through the $O(M^{\frac{3}{2}})$ curvature of the basic state in the general case when the wall curvature is not proportional to $1/(2x)^{\frac{3}{4}}$. Thus only when the wavenumber a is as large as of order $M^{\frac{3}{8}}$ do non-parallel effects become negligible and the following asymptotic expression for the neutral Görtler number can be obtained:

$$G = \frac{2BM^{\frac{3}{2}}}{\kappa(x_n)(2x_n)^{\frac{3}{2}}} + g_0 a^4 + a^3 \frac{1}{(2x_n)^{\frac{1}{4}}} \left(\frac{3g_0}{2\hat{T}_0^2} \frac{\partial^2 g_0}{\partial \eta^{*2}} \right)^{\frac{1}{2}} + \ldots, \tag{3.1}$$

where
$$B \stackrel{\text{def.}}{=} \lim_{M\to\infty} M^{-\frac{3}{2}} \int_0^\infty \bar{T}(\eta)\,\mathrm{d}\eta, \quad g_0 = -\frac{2(2x_n)^{\frac{1}{2}} \bar{\mu}_0^2 \hat{T}_0^4}{\sigma\kappa(x_n)\,\hat{T}_1}, \tag{3.2}$$

and $\hat{T}_0 = \hat{T}(\eta^*)$, $\hat{T}_1 = T'(\eta^*)$, $\bar{\mu}_0 = \bar{\mu}(\hat{T}_0)$. The constant η^* denotes the centre of vortex activity and has the numerical value of 3.001 when $\sigma = 0.72$, $m = 0.509$, whilst x_n is the neutral position. In (3.1) the first term is due to the curvature of the basic state and other terms are due to viscous effects. It is clear that $a = O(M^{\frac{3}{8}})$ is the order at which viscous effects become comparable with the effects of centrifugal acceleration due to the curvature of the basic state.

Equation (3.1) is a relation between the neutral Görtler number G, the wavenumber a and the neutral position x_n. In theory this relation can be inverted to give an expression for x_n as a function of G and a. Thus for a given Görtler number and wavenumber, we know where the vortices will become neutrally stable. After the neutral position has been determined, our next task is to investigate how Görtler vortices will grow beyond the neutral position. This task was taken up in the nonlinear theory presented in Fu & Hall (1992). It is shown there that initially at the neutral position Görtler vortices are trapped in a thin viscous layer of $O(\epsilon^{\frac{1}{3}})$ thickness (due to their small-wavelength nature); but as they evolve downstream of the neutral position they spread into the temperature adjustment layer and develop into a large-amplitude vortex structure. This structure consists of a core region of vortex activity bounded by two viscous transition layers where Görtler vortices are forced to decay to zero exponentially. The total flow is written as

$$u = \bar{u} + \frac{1}{M_1} U, \quad v = \bar{v} + V, \quad w = W, \quad p = p + \frac{1}{R}(\tilde{p} + P), \quad T = \bar{T} + \theta. \tag{3.3}$$

Here $(\bar{u}, \bar{v}, \bar{p} + \tilde{p}/R, \bar{T})$ is the mean flow; whilst $(U/M_1, V, W, P, \theta)$ is the harmonic part of Görtler vortices. The mean velocity components $\bar{u}$ and $\bar{v}$ have the following expressions:

$$\bar{u} = \frac{\partial f(x,\eta)}{\partial \eta}, \quad \bar{v} = \frac{1}{(2x)^{\frac{1}{2}}}\left\{ -\bar{T}(x,\eta) f + \frac{\partial f}{\partial \eta} I(\bar{T}) \right\} + v_\delta(x,\eta). \tag{3.4a, b}$$

Here, in analogy with (2.30) and (2.31), $f(x,\eta)$ and $\bar{T}(x,\eta)$ expand as

$$f(x,\eta) = \eta - \frac{\beta}{M^{\frac{1}{2}}} + \frac{\bar{f}(x,\eta)}{M_1} + \dots, \quad \bar{T} = \bar{T}(x,\eta) + \dots. \tag{3.5}$$

Equations (3.4) are similar to (2.10) except that f and $\bar{T}$ in (3.4) are also functions of x. This is because after the basic state has been reinforced by nonlinear interaction, it can no longer be described by the similarity variable η alone. Naturally, if v_δ is not present in (3.4b), we do not expect $\bar{u}$ and $\bar{v}$ given by (3.4) to satisfy the continuity equation. Thus the function $v_\delta(x,\eta)$ in (3.4b) is added so that the continuity equation could be satisfied. The function $I(\bar{T})$ in (3.4b) is the integration of the mean temperature from 0 to η (thus the wall-layer temperature is also involved). The explicit expressions for it and v_δ can be found in Fu & Hall (1992). We do not write them out here since they are not needed in the following analysis. The similarity variable $\eta = \eta(x,y)$ is defined by

$$\eta = \frac{1}{(2x)^{\frac{1}{2}}} \int_0^y \frac{\mathrm{d}y}{\bar{T}(x,\eta(x,y))}, \tag{3.6}$$

where the function $\bar{T}$ in the integrand is understood to be the composite solution of the mean temperature (i.e. the wall-layer temperature and the mean temperature in the temperature adjustment layer). In the following analysis, it is $\partial\bar{f}/\partial\eta$ (not $\bar{u}$) that will appear. For convenience, we shall refer to it as the mean streamwise velocity component although it is only the $O(1/M_1)$ correction term in the expression for $\bar{u}$.

In the core region of vortex activity, the mean flow part and the harmonic part of the flow have the following forms of solution:

$$\left.\begin{aligned}
&\bar{f} = \bar{f}_0(x,\eta)+\epsilon\bar{f}_1(x,\eta)+\ldots, \quad \bar{T}(x,\eta) = \bar{T}_0(x,\eta)+\epsilon\bar{T}_1(x,\eta)+\ldots,\\
&v_\delta = v_\delta^0(x,\eta)+\epsilon v_\delta^1(x,\eta)+\ldots,\\
&U = \epsilon\{E(U_0^1+\epsilon U_1^1+\ldots)+\epsilon E^2(U_0^2+\ldots)+\ldots+\text{c.c.}\},\\
&V = \epsilon^{-1}\{E(V_0^1+\epsilon V_1^1+\ldots)+\epsilon E^2(V_0^2+\ldots)+\ldots+\text{c.c.}\},\\
&W = \{E(W_0^1+\epsilon W_1^1+\ldots)+\epsilon E^2(W_0^2+\ldots)+\ldots+\text{c.c.}\},\\
&P = \epsilon^{-1}\{E(P_0^1+\epsilon P_1^1+\ldots)+\epsilon E^2(P_0^2+\ldots)+\ldots+\text{c.c.}\},\\
&\theta = \epsilon\{E(\theta_0^1+\epsilon\theta_1^1+\ldots)+\epsilon E^2(\theta_0^2+\ldots)+\ldots+\text{c.c.}\},
\end{aligned}\right\} \tag{3.7}$$

where
$$E = \exp(\mathrm{i}z/\epsilon), \quad \epsilon = 1/a, \tag{3.8}$$

and c.c. denotes the conjugate. It has been shown in Fu & Hall (1992) that the mean flow quantities $\bar{T}_0, \bar{f}_0$ and the fundamental V_0^1 satisfy the following three equations:

$$\frac{\sigma}{\bar{\mu}_0^2\bar{T}_0^4}\frac{\partial\bar{T}_0}{\partial\eta}+\frac{(2x)^{\frac{1}{2}}}{H(x)} = 0, \tag{3.9}$$

$$\frac{\partial}{\partial\eta}\left(\frac{\bar{\mu}_0}{\bar{T}_0}\frac{\partial^2\bar{f}_0}{\partial\eta^2}\right)+\eta\frac{\partial^2\bar{f}_0}{\partial\eta^2}-2x\frac{\partial^2\bar{f}_0}{\partial\eta\,\partial x} = -\frac{2}{\bar{T}_0^2}\frac{\partial}{\partial\eta}\left(\frac{1}{\bar{\mu}_0\bar{T}_0}\frac{\partial^2\bar{f}_0}{\partial\eta^2}|V_0^1|^2\right)-\frac{4(2x)^{\frac{1}{2}}}{\sigma H(x)}\bar{\mu}_0\frac{\partial^2\bar{f}_0}{\partial\eta^2}|V_0^1|^2, \tag{3.10}$$

$$\frac{1}{\sigma}\frac{\partial}{\partial\eta}\left(\frac{\bar{\mu}_0}{\bar{T}_0}\frac{\partial\bar{T}_0}{\partial\eta}\right)+\eta\frac{\partial\bar{T}_0}{\partial\eta}-2x\frac{\partial\bar{T}_0}{\partial x} = \frac{2(2x)^{\frac{1}{2}}}{H(x)}\frac{\partial}{\partial\eta}(\bar{\mu}_0\bar{T}_0|V_0^1|^2). \tag{3.11}$$

Here $H(x)$ is defined by

$$H(x) = BN\left\{\frac{\kappa(x)}{\kappa(x_n)(2x_n)^{\frac{3}{2}}}-\frac{1}{(2x)^{\frac{3}{2}}}\right\}+\tfrac{1}{2}\kappa g_0, \tag{3.12}$$

and $\bar{\mu}_0 = \mu(\bar{T}_0)$. The constant N in (3.12) is given by $N = M^{\frac{3}{2}}a^{-4}$ and is of $O(1)$ since we have assumed that the wavenumber is of order $M^{\frac{3}{8}}$. In our numerical calculations N is taken to be unity.

Equations (3.10) and (3.11) are the 'modified' forms of the basic state equations (2.32) and (2.33). The appearance of the fundamental V_0^1 in the forcing terms on the right-hand sides reflects the fact that the basic state is now completely altered by nonlinear interaction.

The mean flow temperature $\bar{T}_0$ can be first solved from (3.9). We note that as x tends to the neutral position x_n, $\bar{T}_0$ tends to the basic state temperature and (3.9) then reduces to the condition for the Görtler vortices to be neutrally stable at the location $\eta = \eta^*$. The fact that (3,9) is now an equation for determining the mean temperature $\bar{T}_0(x,\eta)$ shows that the mean flow has to adjust itself so that it is neutrally stable to vortices everywhere in the temperature adjustment layer.

After $\bar{T}_0$ has been found, (3.11) can then be solved to determine the fundamental V_0^1 (and hence U_0^1 etc. since they are related to V_0^1). It is easy to show that the result of solving (3.11) is

$$|V_0^1|^2 = \frac{H(x)}{2(2x)^{\frac{1}{2}}\bar{\mu}_0\bar{T}_0}\int^{\eta}\left\{\frac{1}{\sigma}\frac{\partial}{\partial\eta}\left(\frac{\bar{\mu}_0}{\bar{T}_0}\frac{\partial\bar{T}_0}{\partial\eta}\right)+\eta\frac{\partial\bar{T}_0}{\partial\eta}-2x\frac{\partial\bar{T}_0}{\partial x}\right\}\mathrm{d}\eta. \tag{3.13}$$

The two locations where V_0^1 vanishes define the centres $\eta_1(x)$ and $\eta_2(x)$ of the two transition layers. Finally, the solutions in the core region of vortex activity are complete if (3.10) can be solved to give an expression for $\partial\bar{f}_0/\partial\eta$. This has to be done numerically and will be discussed in the next section.

In the two transition layers centred at $\eta = \eta_1(x), \eta_2(x)$, the Görtler vortices are reduced to zero exponentially and so above the upper transition layer and below the lower transition layer, there is only the mean flow. The latter expands as

$$\bar{f} = \tilde{f}_0(x,\eta) + O(\epsilon), \quad \bar{T}(x,\eta) = \tilde{T}_0(x,\eta) + O(\epsilon), \tag{3.14}$$

where $\tilde{f}_0(x,\eta)$ and $\tilde{T}_0(x,\eta)$ satisfy

$$\frac{\partial}{\partial\eta}\left(\frac{\tilde{\mu}_0}{\tilde{T}_0}\frac{\partial^2\tilde{f}_0}{\partial\eta^2}\right) + \eta\frac{\partial^2\tilde{f}_0}{\partial\eta^2} - 2x\frac{\partial^2\tilde{f}_0}{\partial\eta\,\partial x} = 0, \tag{3.15}$$

$$\frac{1}{\sigma}\frac{\partial}{\partial\eta}\left(\frac{\tilde{\mu}_0}{\tilde{T}_0}\frac{\partial\tilde{T}_0}{\partial\eta}\right) + \eta\frac{\partial\tilde{T}_0}{\partial\eta} - 2x\frac{\partial\tilde{T}_0}{\partial x} = 0. \tag{3.16}$$

Here $\tilde{\mu}_0 = \mu(\tilde{T}_0)$ and we note that the governing equation (3.16) for $\tilde{T}_0(x,\eta)$ is decoupled from that for $\tilde{f}_0$. We can therefore solve (3.16) on $[0,\eta_1], [\eta_2,\infty)$ first subject to the appropriate boundary conditions at $\eta = 0, \infty$ and matching conditions at $\eta = \eta_1, \eta_2$ (in order to match with $\bar{T}_0$ given by (3.9). This gives rise to a free boundary problem which has been solved numerically in Fu & Hall (1992) for several curvatures. The reader is referred to that paper for a detailed explanation of the numerical procedure which is used to find the locations of η_1, η_2 and the mean temperature field in the whole region $0 < \eta < \infty$.

In the following section, we shall discuss the numerical solutions of (3.10) and (3.15) since their solution for $\tilde{f}_0$ and $\bar{f}_0$ were not given in Fu & Hall (1992) and will be needed in the solution of the Rayleigh equation in later sections.

4. Numerical solution for the mean streamwise velocity

In this section, we shall outline a numerical scheme which we have used to integrate the partial differential equations (3.10) and (3.15). We see from these two equations that the dependent variables are really $\partial\bar{f}_0/\partial\eta$ and $\partial\tilde{f}_0/\partial\eta$. To simplify notation, we shall denote these two functions by $\bar{f}$ and $\tilde{f}$, respectively, and drop the subscripts '0' on $\bar{T}_0$, $\tilde{T}_0$, $\bar{\mu}_0$ and $\tilde{\mu}_0$ in these two equations. Thus our problem is to integrate

$$\frac{\partial}{\partial\eta}\left(\frac{\bar{\mu}}{\bar{T}}\frac{\partial\bar{f}}{\partial\eta}\right) + \eta\frac{\partial\bar{f}}{\partial\eta} - 2x\frac{\partial\bar{f}}{\partial x} = -\frac{2}{\bar{T}^2}\frac{\partial}{\partial\eta}\left(\frac{1}{\bar{\mu}\bar{T}}\frac{\partial\bar{f}}{\partial\eta}|V_0^1|^2\right) - \frac{4(2x)^{\frac{1}{2}}}{\sigma H(x)}\bar{\mu}\frac{\partial\bar{f}}{\partial\eta}|V_0^1|^2, \tag{4.1}$$

on $[\eta_1,\eta_2]$ and

$$\frac{\partial}{\partial\eta}\left(\frac{\tilde{\mu}}{\tilde{T}}\frac{\partial\tilde{f}}{\partial\eta}\right) + \eta\frac{\partial\tilde{f}}{\partial\eta} - 2x\frac{\partial\tilde{f}}{\partial x} = 0, \tag{4.2}$$

on $(0,\eta_1]$ and $[\eta_2,\infty)$. Here the mean temperature $\bar{T}$ and $\tilde{T}$, η_1 and η_2 are already known from the solution of the free boundary problem discussed in Fu & Hall (1992).

The appropriate boundary conditions are

$$\tilde{f} \to 0 \quad \text{as} \quad \eta \to \infty, \qquad \tilde{f} \to -\frac{3D}{\sigma\eta^{1+3/\sigma}} + \dots \quad \text{as} \quad \eta \to 0, \tag{4.3}$$

and matching conditions are

$$\left.\begin{aligned} \tilde{f}(x,\eta_1) &= \bar{f}(x,\eta_1), \quad \tilde{f}(x,\eta_2) = \bar{f}(x,\eta_2),\\ \frac{\partial \tilde{f}}{\partial \eta}(x,\eta_1) &= \frac{\partial \bar{f}}{\partial \eta}(x,\eta_1), \quad \frac{\partial \tilde{f}}{\partial \eta}(x,\eta_2) = \frac{\partial \bar{f}}{\partial \eta}(x,\eta_2). \end{aligned}\right\} \tag{4.4}$$

The interval $(0,\infty)$ is divided into three sub-intervals:

$$\Gamma_1:(0,\eta_1), \quad \Gamma_2:(\eta_1,\eta_2), \quad \Gamma_3:(\eta_2,\infty).$$

Our aim now is to integrate (4.1) in the interval Γ_2 and (4.2) in the intervals Γ_1 and Γ_3 using a marching procedure in the streamwise direction. At each x, we iterate on the values of $\bar{f}(x,\eta_1)$ and $\bar{f}(x,\eta_2)$ so that the matching conditions can be satisfied.

For the purpose of our numerical calculations, it is necessary to work with fixed boundaries so in Γ_1, Γ_2 and Γ_3 we make the transformations

$$\eta = \eta_1(x)\,\mathrm{e}^{\phi}, \quad \eta = \eta_1+\zeta(\eta_2-\eta_1), \quad \eta = \eta_2(x)\,\psi, \tag{4.5a–c}$$

respectively, so that the intervals Γ_1, Γ_2 and Γ_3 now become

$$\Gamma_1^{\phi}:(-\infty,0), \quad \Gamma_2^{\zeta}:(0,1), \quad \Gamma_3^{\psi}:(1,\infty). \tag{4.6}$$

The additional exponential stretching in (4.5a) is introduced to accommodate the rapid change of $\tilde{f}$ near $\eta = 0$ (as indicated by (4.3)).

In terms of the new variables ϕ, ζ and ψ, the governing equations for the three intervals become

$$2x\frac{\partial \tilde{f}}{\partial x}+A_1(x,\phi,\tilde{f})\frac{\partial^2 \tilde{f}}{\partial \phi^2} = B_1\left(x,\phi,\tilde{f},\frac{\partial \tilde{f}}{\partial \phi}\right)\frac{\partial \tilde{f}}{\partial \phi} \quad \text{in} \quad \Gamma_1^{\phi}, \tag{4.7}$$

$$2x\frac{\partial \bar{f}}{\partial x}+A_2(x,\phi,\bar{f})\frac{\partial^2 \bar{f}}{\partial \zeta^2} = B_2\left(x,\zeta,\bar{f},\frac{\partial \bar{f}}{\partial \zeta}\right)\frac{\partial \bar{f}}{\partial \zeta} \quad \text{in} \quad \Gamma_2^{\zeta}, \tag{4.8}$$

$$2x\frac{\partial \tilde{f}}{\partial x}+A_3(x,\psi,\tilde{f})\frac{\partial^2 \tilde{f}}{\partial \psi^2} = B_3\left(x,\psi,\tilde{f},\frac{\partial \tilde{f}}{\partial \psi}\right)\frac{\partial \tilde{f}}{\partial \psi} \quad \text{in} \quad \Gamma_3^{\psi}. \tag{4.9}$$

Here

$$\left.\begin{aligned} A_1 &= -(1+m)\frac{\tilde{T}^{\frac{1}{2}}}{\tilde{T}+m}\frac{\mathrm{e}^{-2\phi}}{\eta_1^2}\\ B_1 &= 1+\frac{2x\eta_1'}{\eta_1}-(1+m)\frac{\tilde{T}^{\frac{1}{2}}}{\tilde{T}+m}\frac{\mathrm{e}^{-2\phi}}{\eta_1^2}+(1+m)\frac{\mathrm{e}^{-2\phi}}{\eta_1^2}\frac{m-\tilde{T}}{2\tilde{T}^{\frac{1}{2}}(\tilde{T}+m)^2}\left(\frac{\partial \tilde{f}}{\partial \phi}\right),\\ A_2 &= -\frac{1}{(\eta_2-\eta_1)^2}\left(\frac{\bar{\mu}}{\bar{T}}+\frac{2}{\bar{\mu}\bar{T}^3}|V_0^1|^2\right),\\ B_2 &= \frac{1}{\eta_2-\eta_1}\left\{\eta+\left(\frac{\bar{\mu}}{\bar{T}}\right)'+\frac{2}{\bar{T}^2}\frac{\partial}{\partial \eta}\left(\frac{|V_0^1|^2}{\bar{\mu}\bar{T}}\right)+\frac{4(2x)^{\frac{1}{2}}}{\sigma H(x)}\bar{\mu}|V_0^1|^2\right\}\\ &\quad +\frac{2x}{\eta_2-\eta_1}(\eta_1'+\zeta(\eta_2'-\eta_1')),\\ A_3 &= -(1+m)\frac{\tilde{T}^{\frac{1}{2}}}{\tilde{T}+m}\frac{1}{\eta_2^2},\\ B_3 &= \left(1+\frac{2x\eta_2'}{\eta_2}\right)\psi+(1+m)\frac{1}{\eta_2^2}\frac{m-\tilde{T}}{2\tilde{T}^{\frac{1}{2}}(\tilde{T}+m)^2}\frac{\partial \tilde{f}}{\partial \psi}. \end{aligned}\right\} \tag{4.10}$$

Equations (4.7)–(4.9) are parabolic partial differential equations, so their solutions can be obtained by a marching procedure. We shall now use the solution of (4.7) as an example to illustrate our numerical scheme. If the value of $\tilde{f}$ is known at $x = \tilde{x}$, then the following scheme is used to determine this function at $\tilde{x}+\tilde{\epsilon}$:

$$2\tilde{x}\frac{\tilde{f}_i^n-\tilde{f}_i}{\tilde{\epsilon}}+A_1(\tilde{x},\phi_i,\tilde{f}_i)\frac{\tilde{f}_{i+1}^n-2\tilde{f}_i^n+\tilde{f}_{i-1}^n}{h^2}=B_1\left(\tilde{x},\phi_i,\tilde{f}_i,\frac{\tilde{f}_{i+1}-\tilde{f}_{i-1}}{2h}\right)\frac{\tilde{f}_{i+1}-\tilde{f}_{i-1}}{2h}, \quad (4.11)$$

where h is the vertical grid spacing, a superscript 'n' signifies evaluation at the new position $\tilde{x}+\tilde{\epsilon}$ and a subscript signifies evaluation at the indicated vertical grid point. If we replace $-\infty$ by ϕ_0 and use n mesh points in the η-direction, we have

$$\phi_i = \phi_0+ih, \quad \phi_n = \phi_0+nh = 0.$$

Application of (4.11) for $i = 1,2,\ldots,n-1$ gives a triagonal system of equations which can be solved after the following boundary conditions are applied:

$$\tilde{f}_0^n = -\frac{3D}{\sigma(\eta_1\,\mathrm{e}^{\phi_0})^{1+3/\sigma}}, \quad \tilde{f}_n^n = F_1, \quad (4.12)$$

where the value of F_1 is a guess. Then the left derivative of $\tilde{f}$ at $\eta = \eta_1$ can be calculated by using the formula

$$\left.\frac{\partial\tilde{f}}{\partial\eta}\right|_{\eta=\eta_1} = \frac{1}{\eta_1}\left.\frac{\partial\tilde{f}}{\partial\phi}\right|_{\phi=0} = \frac{\tilde{f}_{n+1}^n-\tilde{f}_{n-1}^n}{2h\eta_1}. \quad (4.13)$$

Similarly, by making a guess for $\tilde{f}$ (or $\bar{f}$) at $\eta = \eta_2$, say F_2, we can solve (4.8) and (4.9) and calculate the 'right' derivative of $\bar{f}$ at $\eta = \eta_1$, the 'left' derivative of $\bar{f}$ at $\eta = \eta_2$ and the 'right' derivative of $\tilde{f}$ at $\eta = \eta_2$. By defining two functions G_1 and G_2:

$$G_1(F_1,F_2) = \left.\frac{\partial\tilde{f}}{\partial\eta}\right|_{\eta=\eta_1} - \left.\frac{\partial\bar{f}}{\partial\eta}\right|_{\eta=\eta_1},$$

$$G_2(F_1,F_2) = \left.\frac{\partial\bar{f}}{\partial\eta}\right|_{\eta=\eta_2} - \left.\frac{\partial\tilde{f}}{\partial\eta}\right|_{\eta=\eta_2},$$

we can iterate on F_1 and F_2 with the aid of the two-dimensional version of the Newton–Raphson method until G_1 and G_2 become sufficiently small (ensuring that the matching conditions (4.4) are satisfied).

The above procedure shows how to match the values of $\tilde{f}$ and $\bar{f}$ one step forward along the streamwise direction at a given downstream location. The scheme is complete if the values of $\tilde{f}$ and $\bar{f}$ are known at a certain initial position $x = x_0$. Such values are provided by the weakly nonlinear theory, as we show below.

For small $x-x_{\mathrm{n}}$, Görtler vortices are described by the weakly nonlinear theory given in Fu & Hall (1992). It is found there that the mean streamwise velocity $\bar{f}$ (i.e. $\partial\bar{f}_0/\partial\eta$) in the core region of vortex activity may be written as

$$\bar{f} = \hat{f}'(\eta)+\epsilon^{\frac{3}{8}}u_{m0}+\ldots, \quad (4.14)$$

where $\hat{f}$ is the same function as that appearing in (2.30), whilst u_{m0} satisfies the evolution equation

$$\left(\frac{2x_{\mathrm{n}}\hat{T}_0}{\hat{\mu}_0}\frac{\partial}{\partial\tilde{x}}-\frac{\partial^2}{\partial\phi^2}\right)u_{m0} = \frac{2\hat{f}_0''}{\hat{\mu}_0^2\hat{T}_0^2}\frac{\partial(V_0)^2}{\partial\phi}, \quad (4.15)$$

where the scaled variables $(\phi, \tilde{x})$ are related to (x, η) by

$$\phi = \frac{\eta - \eta^*}{\epsilon^{\frac{1}{2}}}, \quad \tilde{x} = \frac{x - x_n}{\epsilon}, \tag{4.16}$$

and $\hat{T}_0 = \hat{T}(\eta^*)$, $\bar{\mu}_0 = \mu(\hat{T}_0)$, $\hat{f}_0'' = f''(\eta^*)$. In the limit $\tilde{x} \to \infty$, it is established in Fu & Hall (1992) that $(V_0)^2$ has the following asymptotic solution:

$$(V_0)^2 = \frac{\bar{\mu}_0^2 \tilde{b}}{8\sigma^2} \frac{3}{2x_n} (1 + 2\tilde{k})\, \tilde{x}(C^2 - \xi^2) + O(\tilde{x}^0), \tag{4.17}$$

where
$$\xi = (4\tilde{a}/\tilde{b})^{\frac{1}{2}} (\phi / \tilde{x}^{\frac{1}{2}}) \tag{4.18}$$

and $\tilde{a}, \tilde{b}, \tilde{k}$ are known constants. The function $(V_0)^2$ vanishes at $\xi = \pm C$ which, through (4.16) and (4.18), gives the locations $\eta = \eta_1, \eta_2$ of the two transition layers in the small $x - x_n$ limit. It can then be deduced that the corresponding asymptotic solution for u_{m0} is of the form

$$u_{m0} = \tilde{x}^{\frac{3}{2}} H(\xi) + O(\tilde{x}^{\frac{1}{2}}). \tag{4.19}$$

On substituting (4.19) into (4.15) and equating the coefficients of $\tilde{x}^{\frac{1}{2}}$, we obtain

$$\frac{\mathrm{d}^2 \hat{H}}{\mathrm{d}\zeta^2} + \frac{\zeta}{2} \frac{\mathrm{d}\hat{H}}{\mathrm{d}\zeta} - \tfrac{3}{2}\hat{H} + \varDelta \zeta = 0, \tag{4.20}$$

where
$$\hat{H}(\zeta) = H(\xi), \quad \zeta = \left(\frac{x_n \hat{T}_0 \tilde{b}}{2\tilde{a}\bar{\mu}_0}\right)^{\frac{1}{2}} \xi, \quad \varDelta = -(1 + 2\tilde{k}) \frac{6\tilde{a}\hat{f}_0''}{2x_n \sigma^2 \hat{T}_0^2} \left(\frac{\bar{\mu}_0}{2x_n \hat{T}_0}\right)^{\frac{3}{2}}. \tag{4.21}$$

The homogeneous form of (4.20) has one solution given by $\hat{H} = \zeta^3 + 6\zeta$; another solution can be obtained by the method of variation of parameters and can be shown to be an even function of ζ. However, based on the numerical results given in Hall (1982), we expect $\hat{H}(\zeta)$ to be an odd of function of ζ. Thus the general solution of (4.20) is given by

$$\hat{H}(\zeta) = \varDelta \zeta + c_1(\zeta^3 + 6\zeta), \tag{4.22}$$

where the constant c_1 is determined by matching (4.22) with the solutions in the two regions above the upper transition layer and below the lower transition layer. In the region above the upper transition layer, there are no Görtler vortices. The expansion (4.19) is retained but now $\hat{H}(\zeta)$ satisfies

$$\frac{\mathrm{d}^2 \hat{H}}{\mathrm{d}\zeta^2} + \frac{\zeta}{2} \frac{\mathrm{d}\hat{H}}{\mathrm{d}\zeta} - \tfrac{3}{2}\hat{H} = 0. \tag{4.23}$$

The solution which is bounded as $\zeta \to \infty$ is

$$\hat{H}(\zeta) = c_2 \exp\left(-\tfrac{1}{8}\zeta^2\right) U(\tfrac{7}{2}, \zeta/\sqrt{2}), \tag{4.24}$$

where c_2 is a disposable constant and U is a parabolic cylinder function. By matching (4.22) with (4.24) at $\xi = C$, it is easy to show that c_1 and c_2 are given by

$$c_1 = -\frac{(1 + c_3)\varDelta}{(3 + c_3)\zeta_c^2 + 6(1 + c_3)}, \quad c_2 = \frac{\exp(\frac{1}{8}\zeta_c^2)\{\varDelta \zeta_c + c_2(\zeta_c^3 + 6\zeta_c)\}}{U(\frac{7}{2}, \zeta_c/\sqrt{2})}, \tag{4.25}$$

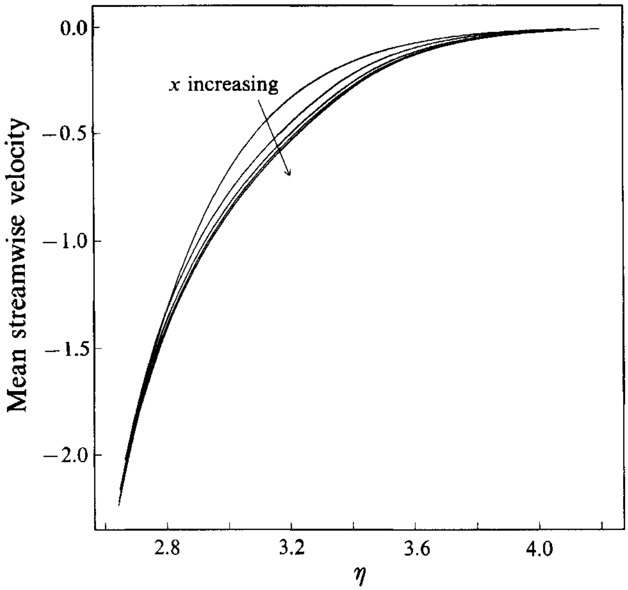

FIGURE 1. Development of the mean streamwise velocity downstream of the neutral position $x_n = 0.3$ over a wall with curvature given by $\kappa(x) = 2x$ for $x = 0.3, 0.55, 0.8, 1.05, 1.3$.

where ζ_c and c_3 can be expressed as

$$c_3 = \zeta_c\left\{\tfrac{1}{2}\zeta_c + \frac{4}{\surd 2}\frac{U(\frac{9}{2}, \zeta_c/\surd 2)}{U(\frac{7}{2}, \zeta_c/\surd 2)}\right\}, \quad \zeta_c = \left(\frac{x_n \hat{T}_0 \tilde{b}}{2\tilde{a}\bar{\mu}_0}\right)^{\frac{1}{2}} C. \tag{4.26}$$

Since $\hat{H}(\zeta)$ should be an odd function of ζ, its solution for $-\infty < \xi \leqslant -C$ can be obtained from (4.24) by replacing ζ by $-\zeta$ and c_2 by $-c_2$, respectively. On collecting the above results together, we have

$$H(\xi) = \hat{H}(\zeta) = \begin{cases} c_2 \exp(-\frac{1}{8}\zeta^2)\, U(\frac{7}{2}, \zeta/\surd 2), & \zeta_c \leqslant \zeta < \infty, \\ \Delta\zeta + c_1(\zeta^3 + 6\zeta), & -\zeta_c \leqslant \zeta \leqslant \zeta_c, \\ -c_2 \exp(-\frac{1}{8}\zeta^2)\, U(\frac{7}{2}, -\zeta/\surd 2), & -\infty < \zeta \leqslant \zeta_c. \end{cases} \tag{4.27}$$

On substituting (4.19) back into (4.14) and making use of (4.16), we obtain the expression

$$\bar{f} = \hat{f}' + (x - x_n)^{\frac{3}{2}} \hat{H}(\zeta) + \ldots, \tag{4.28}$$

which is valid for $x - x_n \ll 1$. Evaluating the first two terms on the right-hand side of (4.28) at some location near x_n then gives the appropriate initial conditions for the partial differential equations (4.7)–(4.9).

In figure 1, we show the evolution of the mean streamwise velocity component downstream of the neutral position $x_n = 0.3$ (note that throughout this section the term 'mean streamwise velocity' is really meant for the $O(1/M_1)$-correction part of the mean streamwise velocity, see the paragraph below (3.6)). The numerical calculation corresponds to the curvature case $\kappa(x) = 2x$ and to an insulated wall without dissociation. The initial condition is obtained by evaluating (4.28) at $x_0 = 0.301$. It is clear from the graph that alteration of the basic state by nonlinear Görtler vortex interaction mainly takes place in the region of Görtler vortex activity and as Görtler vortices develop downstream, they reinforce the basic state by making

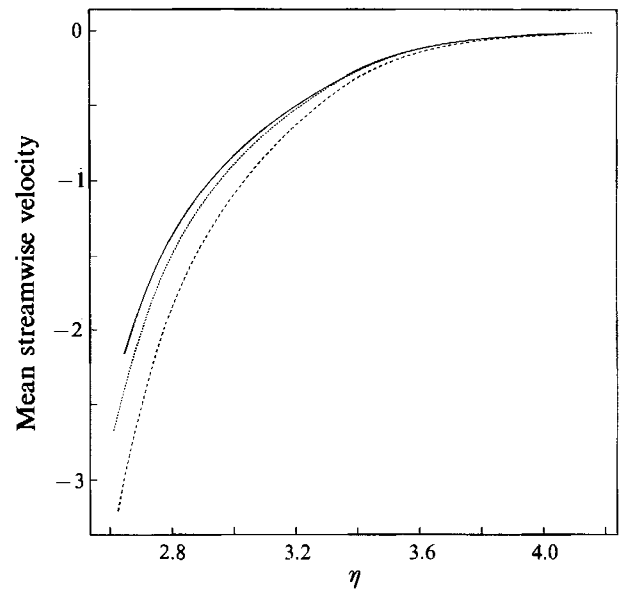

FIGURE 2. Profiles of the mean streamwise velocity after Görtler vortices have evolved a distance of 0.5 downstream of the neutral position $x_n = 0.3$ over a wall with curvature given by $\kappa(x) = 2x$. ——, Ideal gas model (insulated wall); ....., real gas model (insulated wall); ---, ideal gas model (cooled wall, $n = 0.6$).

the mean streamwise velocity grow monotonically. In figure 2, we show the effects of wall cooling and gas dissociation on the development of the mean streamwise velocity by considering three cases: insulated wall with dissociation neglected (case I), insulated wall with dissociation taken into account (case II), and cooled wall ($n = 0.6$) with dissociation neglected (case III). The wall curvature and the initial condition are the same as in figure 1. Initially at the neutral position $x_0 = 0.3$, the amplitude corresponding to case II lies between those for cases I and III (since the values of D have this property and the amplitude is proportional to D). Figure 2 shows that this property is still preserved after Görtler vortices have evolved a distance of 0.5 downstream of the neutral position.

5. Rayleigh secondary instability

After all of the mean flow quantities associated with the large-amplitude Görtler vortex structure have been determined, we are now in a position to study the Rayleigh secondary instability mentioned in the introduction. In order to determine whether Rayleigh secondary instability can really be triggered or not, we superimpose a Rayleigh travelling wave structure on the existing Görtler vortex structure. Thus the total flow is now written as

$$\begin{Bmatrix} u \\ v \\ w \\ p \\ T \\ \rho \end{Bmatrix} = \begin{Bmatrix} \bar{u} \\ \bar{v} \\ 0 \\ 1/(\gamma M^2)+\tilde{p}/R \\ \bar{T} \\ \bar{\rho} \end{Bmatrix} + \begin{Bmatrix} U \\ V \\ W \\ P/R \\ \theta \\ \rho \end{Bmatrix} + \delta \begin{Bmatrix} \tilde{u} \\ R^{\frac{1}{2}}\tilde{v} \\ R^{\frac{1}{2}}\tilde{w} \\ \tilde{p} \\ \tilde{\theta} \\ \tilde{\rho} \end{Bmatrix} \mathrm{e}^{\mathrm{i}R^{\frac{1}{2}}k(x-ct)}. \tag{5.1}$$

Here the three terms represent in turn the mean flow, the harmonic part of Görtler vortices and the Rayleigh travelling wave structure. The small parameter δ is introduced to facilitate linearization and we note that the Rayleigh travelling wave is varying at short length and time scales. We assume the wavenumber k to be real and allow the wave speed c to be complex. The growth rate is then given by $kR^{\frac{1}{2}}$ times the imaginary part of c.

On substituting (5.1) into the governing equations (2.2)–(2.7) and performing the usual linearization with respect to δ, we obtain

$$\mathrm{i}k(\bar{U}-c)\,\tilde{\rho}+\mathrm{i}k\rho^*\tilde{u}+\frac{\partial(\rho^*\tilde{v})}{\partial y}+\frac{\partial(\rho^*\tilde{w})}{\partial z}=0, \tag{5.2}$$

$$\mathrm{i}k(\bar{U}-c)\,\tilde{u}+\tilde{v}\frac{\partial\bar{U}}{\partial y}+\tilde{w}\frac{\partial\bar{U}}{\partial z}=-\frac{1}{\rho^*}\mathrm{i}k\tilde{p}, \tag{5.3}$$

$$\mathrm{i}k(\bar{U}-c)\,\tilde{v}=-\frac{1}{\rho^*}\frac{\partial\tilde{p}}{\partial y}, \tag{5.4}$$

$$\mathrm{i}k(\bar{U}-c)\,\tilde{w}=-\frac{1}{\rho^*}\frac{\partial\tilde{p}}{\partial z}, \tag{5.5}$$

$$\mathrm{i}k(\bar{U}-c)\,\tilde{\theta}+\tilde{v}\frac{\partial\theta^*}{\partial y}+\tilde{w}\frac{\partial\theta^*}{\partial z}=\frac{(\gamma-1)M^2}{\rho^*}\mathrm{i}k(\bar{U}-c)\,\tilde{p}, \tag{5.6}$$

$$\gamma M^2\tilde{p}=p^*\tilde{\theta}+\theta^*\tilde{\rho}, \tag{5.7}$$

where

$$\bar{U}=\bar{u}+U,\quad \rho^*=\bar{\rho}+\rho,\quad \theta^*=\bar{T}+\theta. \tag{5.8}$$

We note from (2.14) that in the temperature adjustment layer where $\alpha=0$, ρ^* and θ^* satisfy the relation $\rho^*\theta^*=1$. By using this relation, we can eliminate $\tilde{u}$, $\tilde{v}$, $\tilde{w}$ and $\tilde{\theta}$ in favour of $\tilde{p}$ in (5.2)–(5.7) and obtain the following single equation for the pressure $\tilde{p}$:

$$\left(\frac{\partial^2}{\partial y^2}+\frac{\partial^2}{\partial z^2}-k^2\right)\tilde{p}+k^2(\bar{U}-c)^2M^2\frac{\tilde{p}}{\theta^*}-\frac{2}{\bar{U}-c}\left(\frac{\partial\bar{U}}{\partial y}\frac{\partial\tilde{p}}{\partial y}+\frac{\partial\bar{U}}{\partial z}\frac{\partial\tilde{p}}{\partial z}\right)+\frac{1}{\theta^*}\left(\frac{\partial\tilde{\theta}^*}{\partial y}\frac{\partial\tilde{p}}{\partial y}+\frac{\partial\tilde{\theta}^*}{\partial z}\frac{\partial\tilde{p}}{\partial z}\right)=0. \tag{5.9}$$

When Görtler vortices are absent, this equation reduces to the well-known Rayleigh equation (see, for example, Cowley & Hall 1990)

$$\frac{\partial^2\tilde{p}}{\partial y^2}+\left(\frac{\bar{T}_y}{\bar{T}}-\frac{2\bar{u}_y}{\bar{u}-c}\right)\frac{\partial\tilde{p}}{\partial y}-k^2\left\{1-\frac{(\bar{u}-c)^2M^2}{\bar{T}}\right\}\tilde{p}=0. \tag{5.10}$$

In view of (5.8), (3.3)–(3.5), (3.7) and (3.14), the functions $\bar{U}$ and θ^* in (5.9) can be expressed as

$$\begin{aligned}\bar{U}&=1+\frac{1}{M_1}\frac{\partial\bar{f}_0}{\partial\eta}+\ldots+\frac{1}{M_1}\{\epsilon E(U_0^1+\ldots)+\ldots\text{c.c.}\},\\ \theta^*&=\bar{T}_0(x,\eta)+\ldots+\epsilon E(\theta_0^1+\ldots)+\ldots+\text{c.c.}\end{aligned} \tag{5.11}$$

in the region $-\eta_1<\eta<\eta_2$, and can be expressed as

$$\bar{U}=1+\frac{1}{M_1}\frac{\partial\tilde{f}_0}{\partial\eta}+\ldots,\quad \theta^*=\tilde{T}_0(x,\eta)+\ldots \tag{5.12}$$

in the regions $-\infty < \eta < \eta_1$ and $\eta_2 < \eta < \infty$. We note that in the latter regions there are no Görtler vortices.

We now look for the following form of solution for (5.9):

$$\tilde{p}(x,y,z) = P_0(x,\eta)+\epsilon^3 P_1(x,\eta,z)+\ldots, \quad c = 1+\frac{\tilde{c}}{M_1}+\ldots. \tag{5.13}$$

By assuming that the leading-order z-dependent term in the expression for $\tilde{p}$ to be of order ϵ^3, we will be able to confine our attention to the discussion of Rayleigh instability associated with the generalized inflexion point of the mean flow and therefore exclude the possible instability associated with the generalized inflexion points in the z-direction due to the presence of Görtler vortices.

On substituting (5.11)–(5.13) into (5.9), making use of (3.6), and keeping only those terms which are of order $\epsilon^0 M^0$, we find that $P_0(x,\eta)$ satisfies

$$\frac{\partial^2 P_0}{\partial \eta^2}-\frac{2\bar{f}_0''}{\bar{f}_0'-\tilde{c}}\frac{\partial P_0}{\partial \eta}-2xk^2\bar{T}_0^2 P_0 = 0 \tag{5.14}$$

in the region $-\eta_1 < \eta < \eta_2$, and

$$\frac{\partial^2 P_0}{\partial \eta^2}-\frac{2\tilde{f}_0''}{\tilde{f}_0'-\tilde{c}}\frac{\partial P_0}{\partial \eta}-2xk^2\tilde{T}_0^2 P_0 = 0 \tag{5.15}$$

in the regions $-\infty < \eta < \eta_1$ and $\eta_2 < \eta < \infty$. Here a prime signifies partial differentiation with respect to η. An investigation of the disturbance equations in the transition layer shows that these layers are passive and that $P_0, P_{0\eta}$ are therefore continuous at $\eta = \eta_1, \eta_2$.

In the remaining part of this section, we shall solve these equations for different mean flows to determine the influence of the presence of Görtler vortices, wall cooling and gas dissociation on the growth rate of Rayleigh modes.

5.1. *The influence of wall cooling and gas dissociation*

In the absence of Görtler vortices, $\bar{f}_0'$ and $\tilde{f}_0'$ reduce to $\hat{f}'(\eta)$, $\bar{f}_0''$ and $\tilde{f}_0''$ reduce to $\hat{f}''(\eta)$ defined in (2.36), whilst $\bar{T}_0$ and $\tilde{T}_0$ reduce to $\hat{T}$ determined by (2.33). Equations (5.14) and (5.15) then become

$$\frac{\partial^2 P_0}{\partial \eta^2}-\frac{2\hat{f}''}{\hat{f}'-\tilde{c}}\frac{\partial P_0}{\partial \eta}-((2x)^{\frac{1}{2}}k)^2\hat{T}^2 P_0 = 0. \tag{5.16}$$

This equation has been solved before by Blackaby *et al.* (1993) for unit Prandtl number without taking gas dissociation into account. Here we shall solve this equation for Prandtl number $\sigma = 0.72$ which is more relevant to air. We shall also study how gas dissociation affects the growth rate.

As we have remarked at the end of §2, properties in the wall layer affect properties in the temperature adjustment layer only through the matching constant D which appears in (2.29). Thus gas dissociation and wall cooling affect Rayleigh instability simply through changing the values of D. We note from (2.36) that the functions $\hat{f}''/D$ and $\hat{f}'/D$ are independent of wall cooling and gas dissociation. It is easily seen from (5.16) that if $\tilde{c}_0$ and D_0 denote the values of $\tilde{c}$ and D when the wall is insulated and gas dissociation is neglected, then for any other situations the value of $\tilde{c}$ is given by

$$\tilde{c} = (D/D_0)\,\tilde{c}_0. \tag{5.17}$$

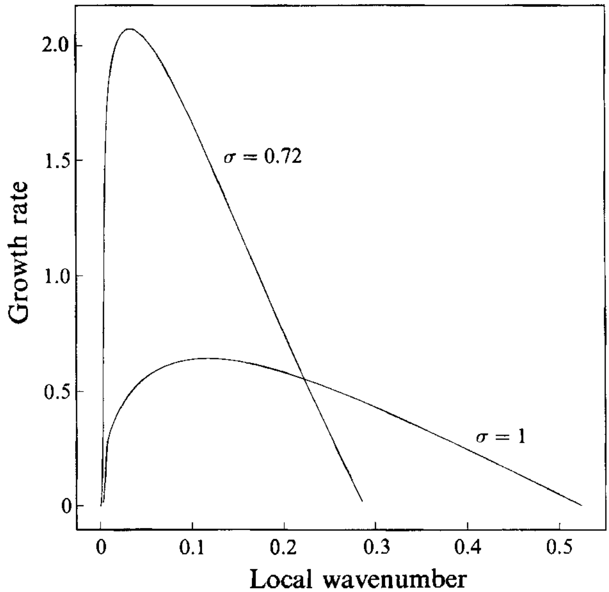

FIGURE 3. A comparison of the growth rate corresponding to $\sigma = 1$ and 0.72 when Görtler vortices are absent.

In table 1, we have given the numerical values of D when the wall is cooled or gas dissociation is taken into account. It is clear that both gas dissociation and wall cooling increase the value of D and thus through (5.17) they increase the growth rate of Rayleigh instability. The D values given in table 1 imply that if the wall is cooled to one-fifth of its insulated temperature, then the growth rate will be more than doubled. Whilst the D values in table 1 imply relatively smaller influence on the growth rate by taking gas dissociation into account, we should note, however, that those values only correspond to one set of parameters associated with gas dissociation (given in the paragraph above (2.37)). In theory the degree of gas dissociation can be 'tuned' by choosing different values for these parameters in our numerical calculation. In particular, the degree of gas dissociation can be increased by choosing a larger value for a and a smaller value for b in (2.18). By (2.17), this is effectively to choose a larger value for the Mach number if the gas properties are fixed. Thus gas dissociation may have a more significant effect on the growth rate than that implied by table 1.

Equation (5.16) has been solved by using a fourth-order Runge–Kutta method to determine the relation between the scaled growth rate (defined as $(2x)^{\frac{1}{2}}k$ times the imaginary part of $\tilde{c}$) and the local wavenumber $(2x)^{\frac{1}{2}}k$. The boundary conditions used are

$$P_0 \sim \frac{1}{\eta^{3/\sigma-1}} \exp\left(\int^{\eta} k\hat{T}\,\mathrm{d}\eta\right) \quad \text{as} \quad \eta \rightarrow 0, \quad \text{and} \quad P_0 \sim \exp\left(-(2x)^{\frac{1}{2}}k\eta\right) \quad \text{as} \quad \eta \rightarrow \infty. \tag{5.18}$$

The results from such a numerical integration are shown in figure 3 and on the same plot we have also shown Blackaby *et al.*'s result for $\sigma = 1$ (note that their wavenumber is $(1+m)^{\frac{1}{2}}$ times the k and their wave speed is $(1-\gamma)$ times the c here). Both curves correspond to an insulated wall with gas dissociation neglected. We can see that when $\sigma = 0.72$ the growth rate attains its maximum value of 2.0735 at a

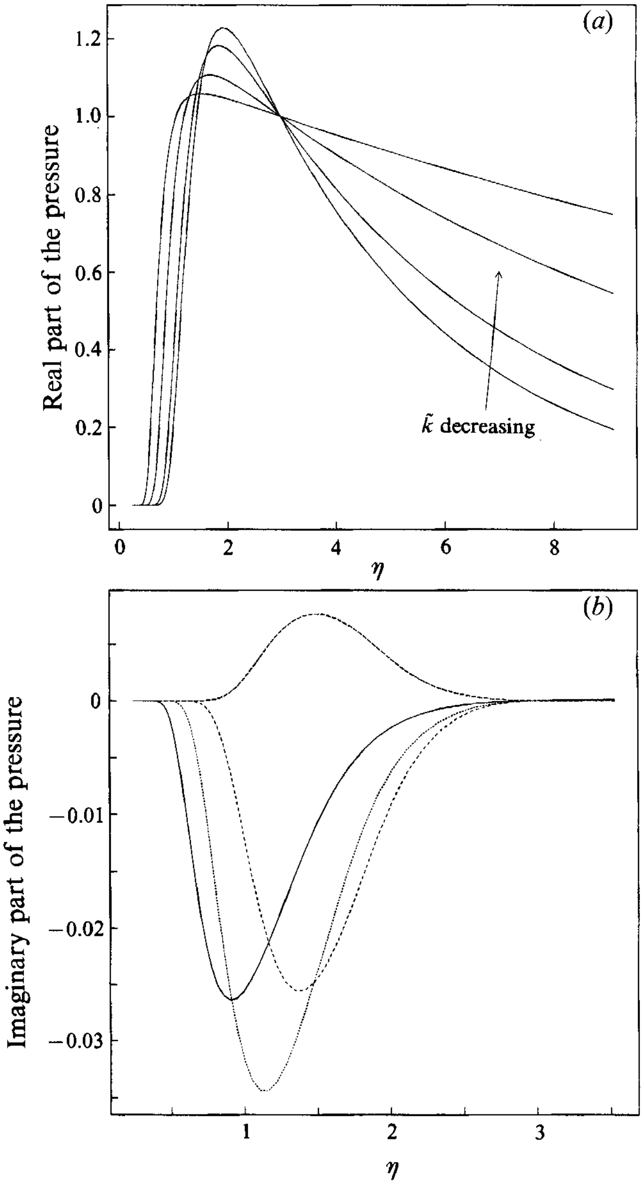

FIGURE 4. (*a*) The real part and (*b*) the imaginary part of the pressure at different values of the wavenumber ($\tilde{k} = (2x)^{\frac{1}{2}}k$) when Görtler vortices are absent, the wall is insulated and gas dissociation is neglected. ——, $\tilde{k} = 0.05$; ....., $\tilde{k} = 0.1$; -----, $\tilde{k} = 0.2$; ——, $\tilde{k} = 0.27$.

smaller wavenumber $(2x)^{\frac{1}{2}}k = 0.034757$ than that for $\sigma = 1$. The maximum growth rate for $\sigma = 0.72$ is roughly four times as large as the maximum growth rate corresponding to $\sigma = 1$. This is not surprising since the growth rate is proportional to D (the proportionality factor being a function of σ as well as the wavenumber); the exact D value for $\sigma = 1$ given by (2.37) when the wall is insulated is only 17 when $m = 0.509$, $\gamma = 1.4$, whilst the corresponding D value for $\sigma = 0.72$ is 186. In figure 4(*a*) and 4(*b*), we show the real and imaginary parts of the pressure for $\sigma = 0.72$ for a range of wavenumbers. We note that whilst the imaginary part of the pressure decays to zero rapidly as $\eta \to 0$ or $\eta \to \infty$, the real part of the pressure decays more

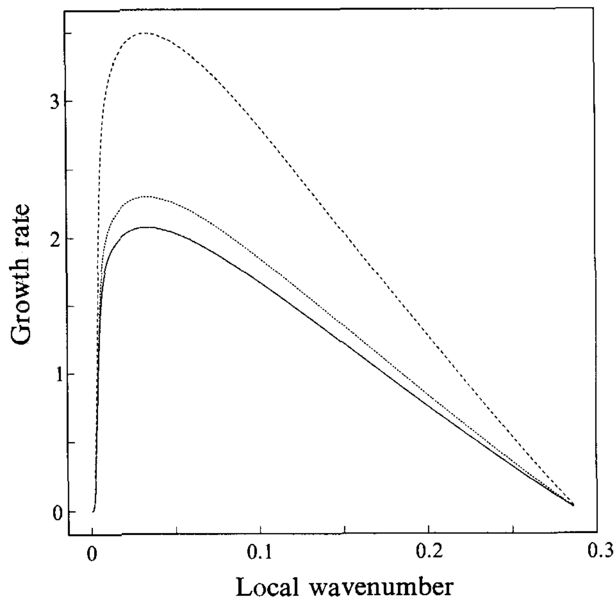

FIGURE 5. Effects of gas dissociation and wall cooling on the growth rate of Rayleigh instability when Görtler vortices are absent and $\sigma = 0.72$. ——, Insulated wall (ideal gas); ....., insulated wall (real gas); ---, cooled wall ($n = 0.4$, ideal gas).

and more slowly towards the edge of the boundary layer as the local wavenumber $\tilde{k}$ $(= (2x)^{\frac{1}{2}}k)$ decreases. These properties can easily be inferred from the decay relations (5.18).

In order to determine the neutral wavenumber, we first note that the generalized inflexion point $\bar{\eta}$ is located where

$$\frac{\partial}{\partial y}\left(\frac{1}{\bar{T}}\frac{\partial \bar{u}}{\partial y}\right) = 0, \quad \text{i.e.} \quad \frac{\hat{f}'''}{\hat{f}''} - \frac{2\hat{T}'}{\hat{T}} = 0. \tag{5.19}$$

Obviously, it is independent of wall cooling or gas dissociation. A simple numerical calculation shows that $\bar{\eta} = 1.958$. Then the neutrally stable Rayleigh mode has $\tilde{c}$ given by

$$\tilde{c} = \hat{f}'(\bar{\eta}) = -18.56. \tag{5.20}$$

The corresponding $(2x)^{\frac{1}{2}}k$ value is obtained by integrating (5.16) over $0 < \eta < \infty$ with an appropriate treatment at the generalized inflexion point. Such a calculation shows that the neutral value of $(2x)^{\frac{1}{2}}k$ is

$$(2x)^{\frac{1}{2}}k = 0.286. \tag{5.21}$$

Finally, in figure 5 we show the effects of gas dissociation and wall cooling on the growth rate in the absence of Görtler vortices. The curve for an insulated wall with gas dissociation neglected is the same as that appearing in figure 3, whilst the other two curves are obtained by using the relation (5.17) and table 1.

5.2. *The influence of Görtler vortices*

As Gortler vortices develop downstream of the neutral position x_n, nonlinear interactions produce an $O(1)$ mean flow correction which completely alters the original basic state. The leading-order mean streamwise velocity $\bar{f}_0'$, $\tilde{f}_0'$ and temperature $\bar{T}_0$, $\tilde{T}_0$ in the Rayleigh equations (5.14) and (5.15) are calculated for any

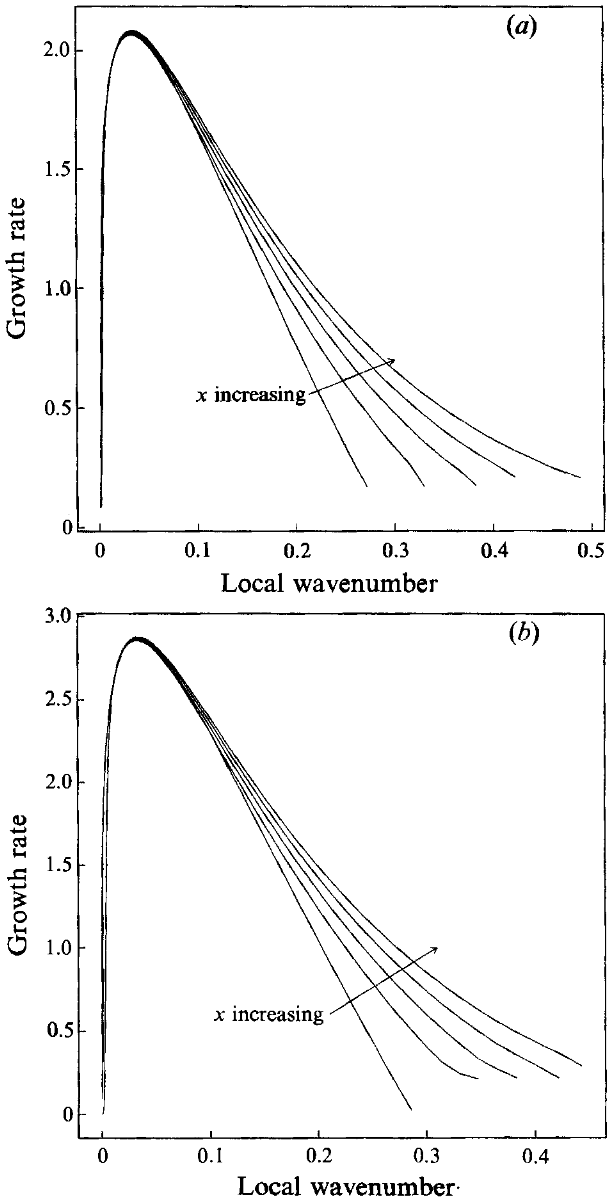

FIG. 6. For caption see page 524.

given x by using the numerical procedures outlined in §4 and Fu & Hall (1992), respectively. The Rayleigh equations (5.14) and (5.15) are then solved to determine the dependence of the growth rate on x (and thus on Görtler vortices). Such results for the curvature case $\kappa(x) = 2x$ are shown in figure 6 (a–c), which in turn correspond to an insulated wall with gas dissociation neglected, a cooled wall ($n = 0.6$) with gas dissociation neglected, and an insulated wall with gas dissociation taken into account. In each of these figures, $x = 0.3$ is the neutral position where there is no Görtler vortex influence. It is clear that the growth rate is increased by the alteration of the basic state by Görtler vortices and as Görtler vortices develop downstream, the growth rate increases monotonically, We have also considered walls with curvatures

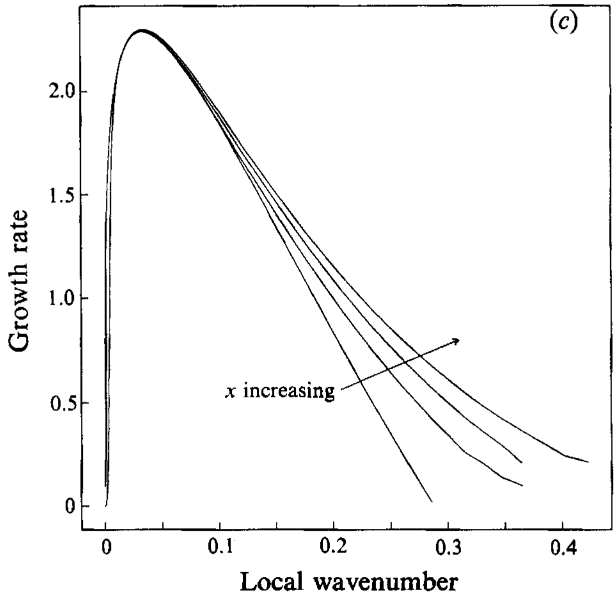

FIGURE 6. Effects of Görtler vortices on the growth rate of Rayleigh instability. (*a*) The wall is insulated with curvature given by $\kappa(x) = 2x$ and gas dissociation is neglected. (*b*) The wall is cooled ($n = 0.6$) with curvature given by $\kappa(x) = 2x$ and gas dissociation is neglected. (*c*) The wall is insulated with curvature given by $\kappa(x) = 2x$ and gas dissociation is taken into account. $x = 0.3$, 0.55, 0.7, 0.85, 1.0 ($x = 0.3$ is the neutral position).

given by $\kappa(x) = (2x)^{\frac{3}{2}}$ and $\kappa(x) = (2x)^{\frac{1}{2}}$. For $\kappa(x) = (2x)^{\frac{3}{2}}$, we obtained similar figures to 6(*a–c*), whilst for $\kappa(x) = (2x)^{\frac{1}{2}}$, we found that for small $x - x_n$, the growth rate is increased by Görtler vortices as the latter evolve downstream, but this increase is hardly noticeable graphically; as Görtler vortices travel further downstream, all growth rate curves coalesce into a single curve. This is because $\kappa(x) = (2x)^{\frac{1}{2}}$ is a special curature case in the sense that at large distances downstream of the neutral position, a similarity solution exists in which the boundaries of the region of vortex activity and the mean flow quantities all become independent of x (and depend only on η, see Fu & Hall 1992).

5.3. *Conclusions*

In summary, we have shown in this paper that the presence of Görtler vortices, wall cooling and gas dissociation all have a destabilizing effect on Rayleigh modes. Although the influence of Görtler vortices is not so pronounced in a small neighbourhood of the neutral position as that of wall cooling or gas dissociation, their existence in a hypersonic boundary layer can nevertheless make the latter more susceptible to Rayleigh modes if they are allowed to travel far enough distances from the neutrally stable position. The main effect of Görtler vortices is to increase the unstable band of Rayleigh waves, thus the presence of large-amplitude vortices is likely to cause the boundary layer to become more receptive to transition induced by Rayleigh modes.

Finally, we conclude with a few remarks concerning the relevance of our calculations to experimental observations. Unfortunately there is as yet no experimental determination of the effects of Görtler vortices, wall cooling and gas dissociation on Rayleigh instabilities. This is of course because of the significant experimental difficulties associated with measuring transition in hypersonic flows. Indeed it is because of these difficulties that the theoretical work was carried out so that some insight into the role of Rayleigh instabilities in the presence of other effects in hypersonic boundary layers might be obtained. However we note that Kendall (1975) has performed experiments at Mach 4.5 and found results in good agreement with the theoretical work on Rayleigh modes. Thus we have some confidence that our results will ultimately be confirmed experimentally.

This research was partially supported by the National Aeronautics and Space Administration under NASA Contract No. BAS1-18605 while P.H. was in residence at the Institute for Computer Applications in Science and Engineering (ICASE), NASA Langley Research Center, Hampton, VA 23665. This work was also supported by USAF under Grant AFOSR89-0042. P.H. is also grateful to SERC for support whilst this work was carried out. The authors wish to thank Dr N. B. Blackaby for help with the calculations of the basic state in the absence of vortices.

REFERENCES

BECKER, E. 1968 *Gas Dynamics*. Academic.

BLACKABY, N., COWLEY, S. & HALL, P. 1993 On the instability of hypersonic flow past a flat plate. *J. Fluid Mech.* **247**, 369–416.

COWLEY, S. J. & HALL, P. 1990 On the instability of hypersonic flow past a wedge. *J. Fluid Mech.* **214**, 17–42.

FU, Y. B. & HALL, P. 1992 Nonlinear development and secondary instability of large amplitude Görtler vortices in hypersonic boundary layers. *Eur. J. Mech.* B **11**, 465–510.

FU, Y. B., HALL, P. & BLACKABY, N. B. 1992 On the Görtler instability in hypersonic flows: Sutherland's law fluids and real gas effects. *Phil. Trans. R. Soc. Lond.* (to appear).

HALL, P. 1982 On the evolution of Görtler vortices in non-parallel boundary layers. *IMA J. Appl. Maths* **29**, 173–196.

HALL, P. & FU, Y. B. 1989 On the Görtler vortex instability mechanism at hypersonic speeds. *Theoret. Comput. Fluid Dyn.* **1**, 125–134.

KENDALL, J. M. 1975 Wind tunnel experiments relating supersonic to hypersonic boundary layer transition. *AIAA J.* **13**, 290–299.

LIGHTHILL, M. J. 1957 Dynamics of a dissociating gas. Part 1. Equilibrium flow. *J. Fluid Mech.* **2**, 1–32.

SMITH, F. T. & BROWN, S. N. 1990 The inviscid instability of a Blasius boundary layer at large values of the Mach number. *J. Fluid Mech.* **219**, 499–518.

STEWARTSON, K. 1964 *The Theory of Laminar Boundary Layers in Compressible Flows*. Clarendon.

SWEARINGEN, J. D. & BLACKWELDER, R. F. 1987 The growth and breakdown of streamwise vortices in the presence of a wall. *J. Fluid Mech.* **182**, 255–290.